

High-performance coherent population trapping clock based on laser-cooled atoms

Xiaochi Liu(刘小赤), Ning Ru(茹宁), Junyi Duan(段俊毅), Peter Yun(云恩学), Minghao Yao(姚明昊), and Jifeng Qu(屈继峰)

Citation: Chin. Phys. B, 2022, 31 (**4**): 043201. DOI: 10.1088/1674-1056/ac2d21
Journal homepage: http://cpb.iphy.ac.cn; http://iopscience.iop.org/cpb

What follows is a list of articles you may be interested in

Light-shift induced by two unbalanced spontaneous decay rates in EIT (CPT) spectroscopies under Ramsey pulse excitation

Xiaoyan Liu(刘晓艳), Xu Zhao(赵旭), Jianfang Sun(孙剑芳), Zhen Xu(徐震), and Zhengfeng Hu(胡正峰)
Chin. Phys. B, 2021, 30 (**8**): 083203. DOI: 10.1088/1674-1056/ac0528

An effective pumping method for increasing atomic utilization in a compact cold atom clock

Xin-Chuan Ouyang(欧阳鑫川), Bo-Wen Yang(杨博文), Jian-Liao Deng(邓见辽), Jin-Yin Wan(万金银), Ling Xiao(肖玲), Hang-Hang Qi(亓航航), Qing-Qing Hu(胡青青), and Hua-Dong Cheng(成华东)
Chin. Phys. B, 2021, 30 (**8**): 083202. DOI: 10.1088/1674-1056/abfccd

Rubidium-beam microwave clock pumped by distributed feedback diode lasers

Chang Liu(刘畅), Sheng Zhou(周晟), Yan-Hui Wang(王延辉), Shi-Min Hou(侯士敏)
Chin. Phys. B, 2017, 26 (**11**): 113201. DOI: 10.1088/1674-1056/26/11/113201

Theoretical investigation on forbidden transition properties of fine-structure splitting in ^{2}D state for K-like ions with $26 \le Z \le 36$

Jian-Peng Liu(刘建鹏), Cheng-Bin Li(李承斌), Hong-Xin Zou(邹宏新)
Chin. Phys. B, 2017, 26 (**10**): 103201. DOI: 10.1088/1674-1056/26/10/103201

Characterizing passive coherent population trapping resonance in cesium vapor cell filled with neon as buffer gas

Liu Zhi, Wang Jie-Ying, Diao Wen-Ting, He Jun, Wang Jun-Min
Chin. Phys. B, 2013, 22 (**4**): 043201. DOI: 10.1088/1674-1056/22/4/043201

High-performance coherent population trapping clock based on laser-cooled atoms

Xiaochi Liu(刘小赤)[1,†], Ning Ru(茹宁)[1], Junyi Duan(段俊毅)[1], Peter Yun(云恩学)[2], Minghao Yao(姚明昊)[1,3], and Jifeng Qu(屈继峰)[1]

[1] *Center for Advanced Measurement Science, National Institute of Metrology, Beijing* 100029, *China*
[2] *National Time Service Center, Chinese Academy of Sciences, Xi'an* 710600, *China*
[3] *College of Metrology and Measurement Engineering, China Jiliang University, Hangzhou* 310018, *China*

(Received 31 August 2021; revised manuscript received 27 September 2021; accepted manuscript online 6 October 2021)

We present a coherent population trapping clock system based on laser-cooled ^{87}Rb atoms. The clock consists of a frequency-stabilized CPT interrogation laser and a cooling laser as well as a compact magneto-optical trap, a high-performance microwave synthesizer, and a signal detection system. The resonance signal in the continuous wave regime exhibits an absorption contrast of $\sim 50\%$. In the Ramsey interrogation method, the linewidth of the central fringe is 31.25 Hz. The system achieves fractional frequency stability of $2.4\times10^{-11}/\sqrt{\tau}$, which goes down to 1.8×10^{-13} at 20000 s. The results validate that cold atom interrogation can improve the long-term frequency stability of coherent population trapping clocks and holds the potential for developing compact/miniature cold atoms clocks.

Keywords: coherent population trapping, atomic clock, cold atoms, microwave synthesizer

PACS: 32.30.–r **DOI:** 10.1088/1674-1056/ac2d21

1. Introduction

Microwave (MW) interrogation can be performed optically in atomic clocks based on coherent population trapping (CPT).[1–3] Thus, no microwave cavity is required in a CPT clock system, and compact, miniature atomic clocks can be developed based on CPT physics.[4–7]

The key component of a typical CPT clock is an alkali atom glass vapor cell. In recent years, vapor-cell-based CPT clocks have demonstrated high short-term frequency stability performance.[8–10] Generally, vapor cells in CPT clocks are filled with buffer gases, such as nitrogen, neon, and argon, to prevent the collision between the alkali atoms and the cell wall. However, the long-term frequency stability of CPT clocks is limited due to pressure- and temperature-dependent shifts, which are introduced by high-pressure buffer gases, as well as resonant light shifts. The resonant light shifts are due to the formation of dark states and the ac Stark shifts when CPT light interacts with alkali atoms.[11–13] The alkali atoms in the vapor cell cannot be completely trapped in the dark state due to ground state decoherence.

The collisional shifts caused by the buffer gases in the vapor cell can be eliminated by performing a CPT clock with laser-cooled atoms.[14–16] The cold atoms can also achieve a long free-evolution time in Ramsey interrogation, which can narrow the linewidth of the central Ramsey fringe and reduce the resonant light shifts. The mitigation of frequency shifts with cold atoms can improve the long-term frequency stability of clocks. As reported in Ref. [15], the resonant light shift could be significantly reduced based on high-coherence excitation fields.

In addition to the collisional and resonant light shifts, the off-resonant light shift needs to be considered as the dominant systematic shift. This shift is caused by the interactions of all detuned energy levels and the light fields. Particularly in CPT clocks, the off-resonant shift strongly depends on the intensity ratio of the two light fields in the CPT interrogation, which are used to couple the hyperfine splitting of the ground states to the excited state in a Λ-system.[17]

This study demonstrates a high-performance Rb CPT atomic clock based on laser-cooled atoms. The atoms are cooled and trapped within three-dimensional compact glass magneto-optical traps (MOTs). An optimized σ_+–σ_- pumping scheme is employed in the CPT interrogation to enhance the atomic population involved in the clock transition. The clock is based on a Ramsey interrogation with a free-evolution time of 16 ms, and the linewidth of the central Ramsey fringe is narrowed to 31.25 Hz. An MW synthesizer with low phase noise and high-power stability is applied in the clock system to suppress the noise via the Dick effect and the intensity ratio fluctuations of the CPT bichromatic light fields.

The remainder of the paper is organized as follows. Section 2 describes the experimental apparatus in detail. Section 3 discusses the Rabi- and Ramsey-type CPT resonance signals and the frequency stability of the cold atom CPT clock. Section 4 present the experimental results and the potential for developing compact high-performance CPT clocks with miniature cold atom physical packages, concluding the paper.

[†]Corresponding author. E-mail: liuxch@nim.ac.cn

© 2022 Chinese Physical Society and IOP Publishing Ltd

2. Experimental setup

The clock is performed with the σ_+–σ_- interrogation,[18,19] which uses alternative left–right circularly polarized counter-propagating beams to couple the hyperfine splitting of the ground states to the excited state in a Λ-system (Fig. 1). This pumping scheme optimizes the atomic population involved in the $m_F = 0$ clock transition and enhances the signal-to-noise ratio of the CPT resonance.

The experimental apparatus of the cold atom CPT clock is shown in Fig. 2. The apparatus can be divided into four main basic blocks defined as laser systems. These systems are a CPT interrogation laser, an optical sideband generation system, a compact MOT system that mainly consists of a cooling light and a vacuum system, and a σ_+–σ_- interrogation and detection system. These blocks are described in detail in the following sections.

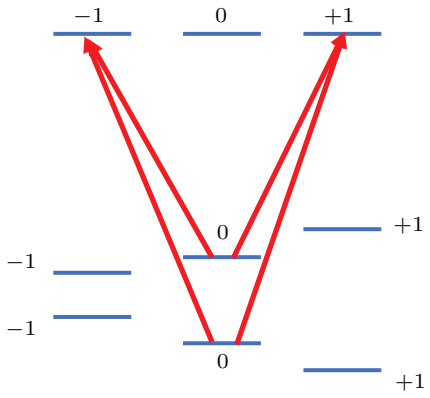


Fig. 1. Scheme of σ_+–σ_- interrogation.

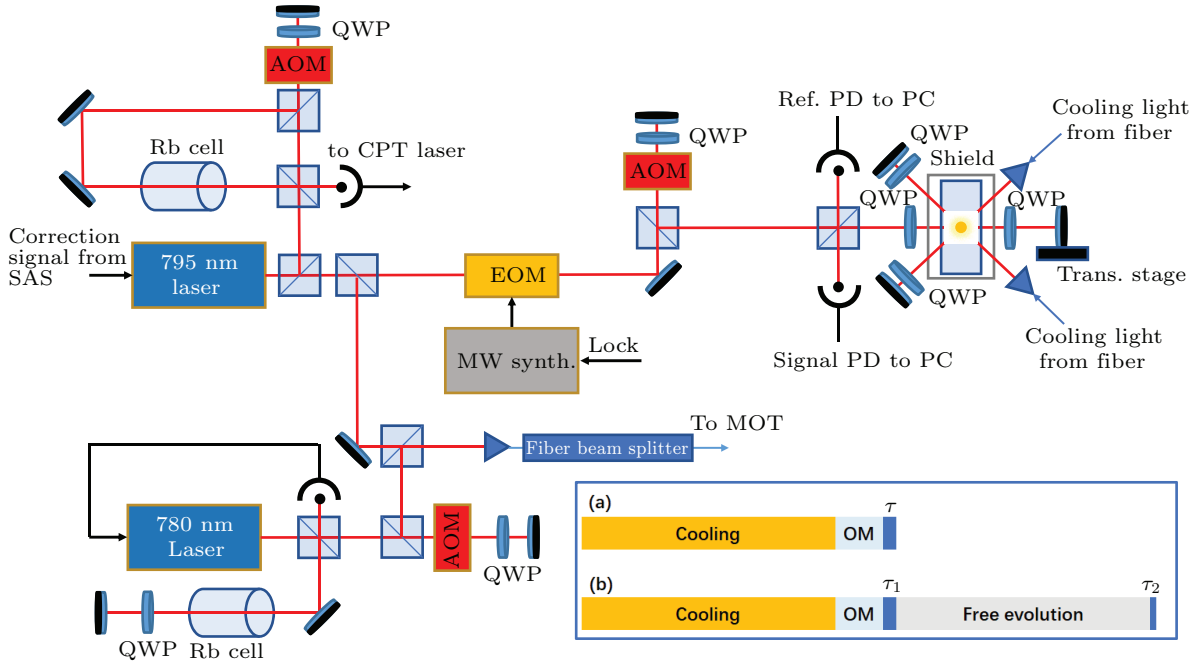


Fig. 2. Architecture of experimental apparatus. SAS: saturated absorption spectroscopy; EOM: electro-optical modulator, AOM: acoustic-optical modulator; MOT: magneto-optical trap; QWP: quarter-wave plate; PD: photodiode; PC: personal computer. OM: optical molasses. Insets: interrogation sequence for (a) continuous wave and (b) pulse mode.

The CPT interrogation laser source is a 1-MHz-width distributed feedback (DFB) laser that is resonant on the ^{87}Rb D_1 line at 795 nm. The laser is frequency-stabilized by saturated absorption spectroscopy (SAS) with an auxiliary vapor cell. The frequency is lock at 160 MHz redshifted from the $|F = 1\rangle$ to $|F' = 1\rangle$ optical transition. The laser frequency is shifted by the double passing of an acousto-optic modulator (AOM). The frequency stability is evaluated by comparing the DFB laser with an optical comb referred to a hydrogen clock. The results are plotted in Fig. 3, which indicate a stability of 5×10^{-12} at 1 s, which changes to 2×10^{-12} at 100 s. The CPT light is split into two beams: one is overlapped with the cooling light as a repump light field for laser cooling, and the other is injected into a pigtailed electro-optical modulator (EOM).

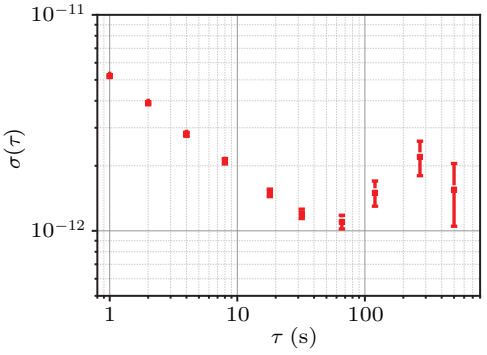


Fig. 3. Frequency stability of CPT interrogation laser.

The cooling light is also stabilized by an SAS technique and detuned by −12 MHz from the ^{87}Rb D_2 optical transition at 780 nm. The vacuum system of the MOT is a 40-cm^3 high-

transmission glass cell connected to a mini-ion pump. The glass cell is surrounded by a pair of anti-Helmholtz coils and a pair of constant-magnetic-field coils. A constant magnetic field of 40 mG is applied parallel to the CPT beam direction. The entire glass cell is isolated from external magnetic perturbations with a double-layer mu-metal shield. The diameter of the cold atoms is 4 mm. Approximately 10^6 atoms are cooled and trapped with the MOT system.

CPT sidebands are created by modulating the monochromatic CPT light with the EOM drive via a 6.834-GHz MW signal. The noise of the relative phase between the CPT sidebands that interrogate the Λ-system of the cold ^{87}Rb atoms can degrade the short- and long-term frequency stability of the clock. Thus, we employ an EOM-based approach, which can generate a much higher coherence optical sideband than the conventional optical phase-locked loop approach by phase-locking a slave laser onto a master laser.

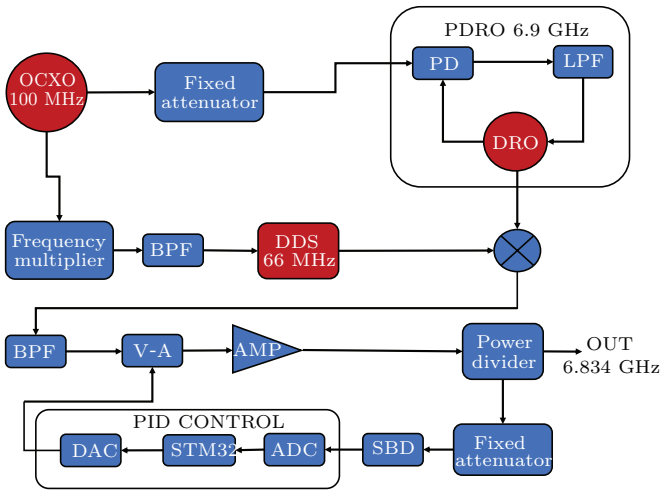


Fig. 4. Basic architecture of a 6.834-GHz microwave synthesizer. OCXO: oven-controlled crystal oscillator; BPF; bandpass filter; LPF: lowpass filter; DDS: direct digital synthesizer; DRO: dielectric resonator oscillator; V-A: voltage control attenuator; DAC: digital-to-analog converter; ADC: analog-to-digital converter; SBD: Schottky barrier diode.

The phase noise of the MW signal can also limit the short-term frequency stability of the CPT clock via the Dick effect.[8,20–23] The frequency stability limitation due to the MW synthesizer is given by

$$\sigma_y^2(\tau) = \frac{1}{\tau}\sum_{i=1}^{\infty}\frac{g_i^2}{g_0^2}\left(\frac{f_m}{\nu_0}\right)^2 S_\varphi(2if_m),$$

where $S_\varphi(f)$ is the power spectral density of phase fluctuations, g presents the sensitivity function, $f_m = \frac{1}{2T_c}$ with T_c is the clock cycle time. A low-phase-noise MW synthesizer is developed in our clock system to satisfy the requirement of the frequency stability. The setup of this custom-built MW synthesizer is shown in Fig. 4. The detailed architecture of this synthesizer was presented in Ref. [24]. The absolute phase noise of the 6.834-GHz output signal with a typical clock cycle time of 21.4 ms (pumping time $\sim$ 1 ms, Ramsey time $\sim$ 20 ms and probe time $\sim$ 0.4 ms, $2f_m = 46.7$ Hz) in our system is -93.6 dBc/Hz (Fig. 5(a)). The calculated frequency-stability limitation due to the Dick effect is 5.85×10^{-14} at 1 s, which is better than the state-of-the-art performance of existing CPT clocks. In the EOM-based CPT clock system, the CPT sideband ratio depends on the output power fluctuation of the MW synthesizer. The theoretical model[17] indicates that the off-resonant light shifts of the CPT clock result from the unstable CPT sidebands ratio, which can limit the long-term frequency stability. Consequently, the output power of the MW synthesizer is also stabilized by a feedback loop. The 6.834-GHz signal is detected and converted to a voltage signal by a Schottky barrier diode detector, and the correction signal is generated by comparing the MW converted voltage with an ultra-stable voltage reference. The output MW signals of the synthesizer in unlocked and locked regimes are shown in Fig. 5(b), which indicates that the MW signal fluctuation is significantly reduced in our synthesizer.

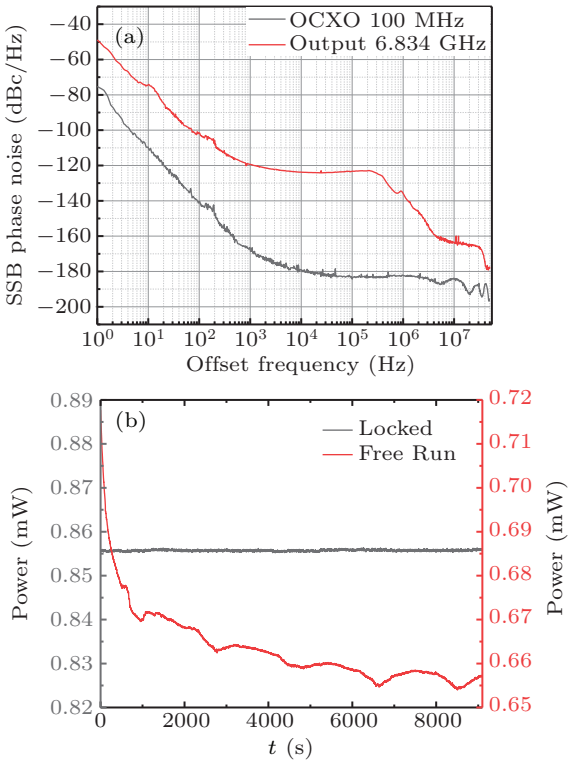


Fig. 5. Performance of the microwave synthesizer. (a) Absolute phase noise of the 100-MHz OCXO (black) and 6.834-GHz output signal (red). (b) Power stability of output signal in free-running regime (black) and stabilized regime (red).

At the output of the EOM, the CPT bichromatic beam is sent to a double-pass AOM. The AOM is driven by an 80-MHz signal and used as an optical switch and an optical intensity stabilizer with a feedback loop. Then, the CPT light field is coupled into a polarization-maintaining fiber and split into two sub-beams via a beam splitter. One sub-beam is sent to the reference photodiode to stabilize the optical intensity

using the previous AOM and feedback loop. The other sub-beam is the CPT interrogation light. The linear polarized CPT light is left-circularly polarized by a quarter-wave plate placed after the beam splitter. The interrogation light propagates through the MOT to interact with the cold atoms. At the other side of the MOT, the beam is reflected after passing through a quarter-wave plate and a mirror fixed onto a translate stage. The σ_+–σ_- interrogation scheme is formed with these counter-propagating circularly polarized beams. The CPT signal amplitude depends on the distance between the cold atoms and the mirror effects due to the interference of the CPT resonance.[18] The position of the translate stage is optimized by maximizing the signal amplitude.

The frequency of the local oscillator is locked onto the central fringe obtained in Ramsey spectroscopy. In our system, the light pulse is generated with the AOM by switching the rf signal. The time sequences of the continuous wave regime and pulse regime are given in the inset of Fig. 2.

In the pulse regime with a switched-on magnetic trap, after a cooling time of ~ 20 ms with the cooling light, the magnetic trap switches off, and the frequency of the cooling light is shifted to form optical molasses. The first CPT pulse τ_1 of 1 ms pumps the atoms into the dark state. Then, a Ramsey time lasts 16 ms with all lights switched off and renders the atoms to evolve freely in the dark. The atoms are probed by another CPT pulse τ_2 of 0.04 ms, which is detected via the signal photodiode. The beam size of the CPT light field is 5 mm, and the optical power is 10 μW.

3. Results

A 7.5 kHz-width CPT signal in a continuous wave regime with the σ_+–σ_- interrogation scheme is shown in Fig. 6(a). The cold atoms and the optimized pumping scheme significantly improve the atomic population trapped in the dark state. The absorption contrast of the cold-atom CPT resonance signal is defined as the ratio of the CPT peak height to the optical absorption and presents the completeness of the dark state formation. The absorption contrast in the proposed system is more than 50%, whereas the absorption contrast of CPT resonance in a vapor cell is typically less than 5%. Thus, the measured result indicates that the formation of the dark state for cold atoms is much better than the atoms in vapor-cell. Ramsey fringes with free-evolution time T_R of 16 ms are plotted in Fig. 6(b). The linewidth of the central Ramsey fringe is 31.25 Hz, which is consistent with the expected value of $1/2T_R$.

The frequency stability of the cold atom CPT clock is traced in Fig. 7 when we lock the LO to the central Ramsey fringe. The frequency stability of the clock is $2.4 \times 10^{-11}/\sqrt{\tau}$ and decreases to 1.8×10^{-13} at 20000 s integration time. The state-of-the-art short-term frequency stability of the vapor cell-based CPT clock is approximately two orders of magnitude higher than that of the cold-atom clock, which is partly due to the fact that the number of atoms interrogated in the vapor cell is three orders of magnitude greater than that in the MOT of the cold-atom CPT clock. However, the frequency stability of the vapor cell-based CPT clock degrades after several hundreds of seconds.

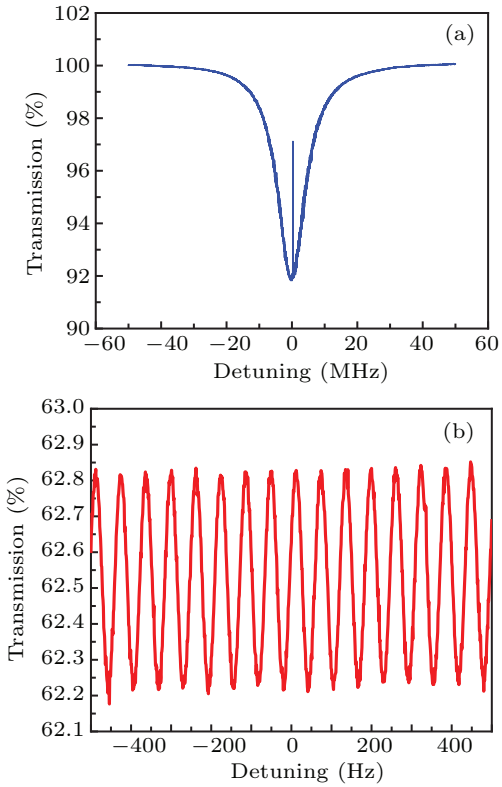


Fig. 6. CPT resonance: (a) continuous-wave interrogation, (b) Ramsey interrogation.

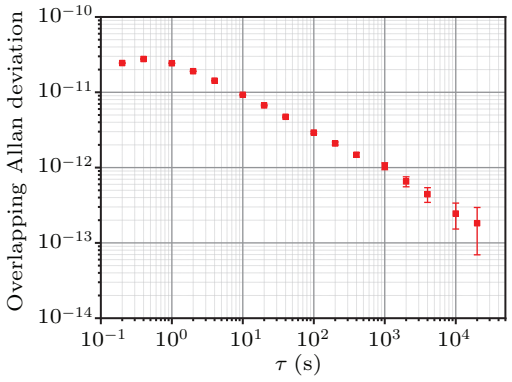


Fig. 7. Frequency stability of the cold-atom CPT clock.

4. Conclusion and perspectives

A CPT clock is a suitable candidate for the development of miniature/compact high-performance atomic clocks. The performance of the conventional vapor cell-based CPT clock is limited by the collisional shift and broadening introduced by high-pressure buffer gases. Here we have demonstrated

a high-performance CPT clock based on laser-cooled atoms. Using the cold-atom technique, the high-pressure shift can be canceled, and the coherence time of the atoms can be significantly increased. The absorption contrast of the detected Rabi-type CPT is $\sim 50\%$, which indicates that the completeness of dark state formation of cold atoms CPT interrogation is much better than that in vapor cell-based interrogation. The free-evolution time of the Ramsey interrogation is up to 20 ms, which corresponds a linewidth of 25 Hz. The frequency stability of the cold-atom CPT clock is $2.4 \times 10^{-11}/\sqrt{\tau}$ and becomes 1.8×10^{-13} at 20000 s. This result validates that the long-term frequency stability of CPT clocks can be greatly improved with cold atoms. However, the physical package of cold atoms demonstrated herein is based on a conventional three-dimensional MOT structure, which is difficult to miniaturize. In the future, we will combine a cold-atom CPT clock system with an MOT based on a grating chip[25–28] to enable us to cool and trap atoms with a single laser beam.

Acknowledgements

We are grateful to Lin Dan and Qiang Hao for their fruitful discussions. This work was supported by the National Natural Science Foundation of China (Grant No. 61975194).

References

[1] Alzetta G, Gozzini A, Moi L and Orriols G 1976 *Nuovo Cimento B* **36** 5

[2] Arimondo E 1996 *Prog. Opt.* **35** 257

[3] Vanier J 2005 *Appl. Phys. B* **81** 421

[4] Knappe S, Shah V, Schwindt P D D, Hollberg L, Kitching J, Liew L A and Moreland J 2004 *Appl. Phys. Lett.* **85** 1460

[5] Lutwak R, Vlitas P, Varghese M, Mescher M, Serkland D K and Peake G M 2005 *Proceedings of the 2005 IEEE International Frequency Control Symposium and Exposition*, August 29–31, 2005, Vancouver, BC, Canada, p. 6

[6] CSAC specifications at www.microsemi.com (2019)

[7] Cash P, Krzewick W, Machado P, Overstreet K R, Silveira M, Stanczyk M, Taylor D and Zhang X 2018 *uropean Frequency and Time Forum (EFTF)*, April 10–12, 2018, Turin, Italy, pp. 65–71

[8] Danet J M, Lours M, Guérandel S and de Clercq E 2014 *IEEE Trans. Ultrason. Ferroelectr. Freq. Control* **61** 567

[9] Yun P, Tricot F, Calosso C E, Micalizio S, Francois B, Boudot R, Guérandel S and de Clercq E 2017 *Phys. Rev. Appl.* **7** 014018

[10] Hafiz M, Coget G, Yun P, Guérandel S, de Clercq E and Boudot R 2017 *J. Appl. Phys.* **121** 104903

[11] Zhu M and Cutler L S 2000 *Proceedings of the 32th Annual Precise Time and Time Interval Systems and Applications Meeting*, November 28–30, 2000, Reston, Virginia, pp. 311–324

[12] Hemmer P R, Shahriar M S, Natoli V D and Ezekiel S 1989 *J. Opt. Soc. Am. B* **6** 1519

[13] Shahriar M S, Hemmer P R, Katz D P, Lee A and Prentiss M G 1997 *Phys. Rev. A* **55** 2272

[14] Blanshan E, Rochester S M, Donley E A and Kitching J 2015 *Phys. Rev. A* **91** 041401

[15] Liu X, Ivanov E, Yudin V I, Kitching J and Donley E A 2017 *Phys. Rev. Appl.* **8** 054001

[16] Liu X, Yudin V I, Taichenachev A V, Kitching J and Donley E A 2017 *Appl. Phys. Lett.* **111** 224102

[17] Pollock J W, Yudin V I, Shuker M, Basalaev M Yu, Taichenachev A V, Liu X, Kitching J and Donley E A 2018 *Phys. Rev. A* **98** 053424

[18] Taichenachev A V, Yudin V I, Velichansky V L, Kargapoltsev S V, Wynands R, Kitching J and Hollberg L 2004 *JETP Lett.* **80** 236

[19] Kargapoltsev S V, Kitching J, Hollberg L, Taichenachev A V, Velichansky V L and Yudin V I 2004 *Laser Phys. Lett.* **1** 495

[20] Dick G J 1989 *Proceedings of the 19th Annual Precise Time and Time Interval Systems and Applications Meeting*, December 1987, Redondo Beach, California, pp. 133–147

[21] Caloss C E, Gozzelino M, Godone A, Lin H and Micalizio S 2020 *IEEE Trans. Ultrason. Ferroelectr. Freq. Control* **67** 1074

[22] Audoin C, Canderlier V and Dimarcq N 1991 *IEEE Trans. Instrum. Meas.* **40** 121

[23] Santarelli G, Audoin C, Makdissi A, Laurent P, Dick G J and Clairon A 1998 *IEEE Trans. Ultrason. Ferroelect. Freq. Control* **45** 887

[24] Yao M, Duan J, Wang X, Han Q, Shi Y, Zhou K, Ru N, Yun P and Liu X 2021 *IEEE Access* **10** 3177

[25] Nshii C C, Vangeleyn M, Cotter J P, Griffin P F, Hinds E A, Ironside C N, See P, Sinclair A G, Riis E and Arnold A S 2013 *Nat. Nanotechnol.* **8** 321

[26] McGilligan J P, Griffin P F, Elvin R, Ingleby S J, Riis E and Arnold A S 2017 *Sci. Rep.* **7** 384

[27] Vangeleyn M, Griffin P F, Riis E and Arnold A S 2009 *Opt. Express* **17** 13601

[28] Vangeleyn M, Griffin P F, Riis E and Arnold A S 2010 *Opt. Lett.* **35** 3453